CENTER FOR COMPUTATIONAL MATHEMATICS REPORTS

University of Colorado at Denver
P.O. Box 173364, Campus Box 170
Denver, CO 80217-3364

Fax: (303) 556-8550
Phone: (303) 556-8442
http://www-math.cudenver.edu/

September 1996 UCD/CCM Report No. 88

Residual-Free Bubbles for the Helmholtz Equation

Leopoldo P. Franca, Charbel Farhat,
Antonini P. Macedo and Michel Lesoinne

September 1996 **UCD/CCM Report No. 88**

RESIDUAL-FREE BUBBLES FOR THE HELMHOLTZ EQUATION

by

Leopoldo P. Franca
Department of Mathematics
University of Colorado at Denver
P.O.Box 173364, Campus Box 170
Denver, CO 80217-3364

Charbel Farhat, Antonini P. Macedo and Michel Lesoinne
Department of Aerospace Engineering Sciences
and Center for Aerospace Structures
University of Colorado at Boulder
Boulder, CO 80309-0429

Abstract

The Galerkin method enriched with residual-free bubbles is considered for approximating the solution of the Helmholtz equation. Two-dimensional tests demonstrate the improvement over the standard Galerkin method and the Galerkin-least-squares method using piecewise bilinear interpolations.

Preprint
July 1996, revised September 1996

1. INTRODUCTION

The discretization of the Helmholtz equation presents distinct numerical problems. This equation models wave propagation and its exact solution is, to a certain extent, oscillatory. Oscillations have warned numerical analysts of limitations in discretization procedures in other contexts, such as in advective dominated flows and bending of thin structures. Here, oscillations are physical and they should be captured accurately avoiding spurious noise from standard numerical methods. When applying the standard Galerkin method using piecewise linear polynomials, the numerical solutions tend to be inaccurate from moderate to large wave numbers within reasonable mesh sizes, pointing out the inadequacy of the use of this method for this application.

Recently, there has been renewed interest in exploring alternative discretization procedures for the Helmholtz equation. We would like to mention, in particular, the work of Harari and Hughes [8] based on the Galerkin-least-squares method (GLS) introduced in the late 80's (see [4,10,11] and references therein). The method seems to be effective in multi-dimensions for this application even if designed for one-dimensional models. However it is no panacea, and for certain wave numbers, geometry, and a reasonable mesh, it may still yield inaccurate solutions. There are certainly other numerical methods available for this equation that may be of interest (e.g., see [1]).

In this paper we apply the residual-free bubbles approach (see [3, 5-7]) to the Helmholtz equation. The residual-free bubbles method is based on the Galerkin formulation employing subspaces spanned by piecewise linear polynomials, and bubble functions that solve exactly a differential equation with loads given by the residuals using piecewise linears. This systematic procedure has shed light in explaining the effectiveness of several numerical "tricks" such as streamline upwinding, mass lumping and selective reduced integration [5-7]. In the Helmholtz equation framework, in the absence of a clear "optimal" method, it offers a potentially high accurate methodology. A related method was proposed independently by Hughes [9], shown equivalent to residual-free bubbles in [2], and applied to this equation in [12].

In the next section we describe the residual-free bubbles method and its application to the Helmholtz equation. In Section 3 we perform numerical experiments and contrast the present method with the Galerkin method and the Galerkin-least-squares method using piecewise linears. We draw conclusions in Section 4.

2. RESIDUAL-FREE BUBBLES FOR THE HELMHOLTZ EQUATION

Let us consider an abstract boundary-value problem given by

$$\begin{aligned} Lu &= f \qquad \text{in}\, \Omega\,, \\ u &= 0 \qquad \text{on}\, \Gamma = \partial\Omega\,, \end{aligned} \tag{1}$$

where L is a differential operator, u is the unknown function and f is a given source function. To define residual free bubbles we consider the standard Galerkin method for (1), i.e., we wish to find $u_h \in V_h$ such that

$$a(u_h, v_h) = (Lu_h, v_h) = (f, v_h) \qquad \forall v_h \in V_h\,. \tag{2}$$

Here u_h and v_h are members of the space of functions V_h which is spanned by piecewise polynomials plus bubble functions, i.e.,

$$u_h = u_1 + u_b\,, \tag{3}$$

where the bubble functions satisfy the differential equations strongly in each element K, i.e.,

$$Lu_b = -(Lu_1 - f) \qquad \text{in}\, K\,, \tag{4}$$

subject to zero Dirichlet boundary condition on the element boundary, i.e.,

$$u_b = 0 \qquad \text{on}\, \partial K\,. \tag{5}$$

The problem defined by equations (4)-(5) is addressed by solving instead

$$L\varphi_{i,K} = -L\psi_{i,K} \qquad \text{in}\, K\,, \tag{6}$$

$$\varphi_{i,K} = 0 \qquad \text{on}\, \partial K\,, \tag{7}$$

where the $\psi_{i,K}$'s are the local basis functions for u_1 and

$$L\varphi_{f,K} = f \qquad \text{in}\, K\,, \tag{8}$$

$$\varphi_{f,K} = 0 \qquad \text{on}\, \partial K\,. \tag{9}$$

Thus, if $u_{1|K} = \sum_{i=1}^{n_{en}} c_{i,K}\psi_{i,K}$, where n_{en} is the number of nodes per element, then

$$u_{b|K} = \sum_{i=1}^{n_{en}} c_{i,K}\varphi_{i,K} + \varphi_{f,K}\,, \tag{10}$$

with the same coefficients $c_{i,K}$'s.

We now wish to address how the bubble function part affects the piecewise linear part of the solution. To this end we use *static condensation*: first we set $v_h = v_{b,K}$ on K (zero elsewhere) in (2) to obtain

$$a(u_1 + u_b, v_{b,K})_K = (f, v_{b,K})_K\,. \tag{11}$$

But this equation is satisfied automatically due to our choice of bubbles. Indeed this equation is the variational equation for

$$Lu_b = -(Lu_1 - f) \qquad \text{in}\, K\,, \tag{12}$$

using $v = v_{b,K}$ on K (zero elsewhere) as test functions.

The second part of static condensation consists in setting $v_h = v_1$ in (2), which gives

$$a(u_1 + u_b, v_1) = (f, v_1)\,, \tag{13}$$

$$a(u_1, v_1) + a(u_b, v_1) = (f, v_1)\,. \tag{14}$$

Hence, using bubbles is equivalent to modifying the variational formulation in the left hand side by the addition of $a(u_b, v_1)$. The residual free bubble method consists in solving (6)-(9) first, then adopting (14).

We now turn to the application of this methodology to the solution of the Helmholtz equation. For this equation we have

$$L = \Delta + k^2 I\,, \tag{15}$$

where k is the wave number, and I is the identity operator. Herein we consider boundary conditions of the type:

$$u = g \qquad \text{on}\,\Gamma_1\,, \tag{16}$$

$$\frac{\partial u}{\partial n} = h \qquad \text{on}\,\Gamma_2\,, \tag{17}$$

where $\partial\Omega = \Gamma_1 \cup \Gamma_2$. Substituting into (14), and integrating by parts, leads to

$$-(\nabla u_1, \nabla v_1) + k^2(u_1, v_1) + \sum_K k^2(u_b, v_1)_K = (f, v_1) - (h, v_1)_{\Gamma_2}\,. \tag{18}$$

From eq. (10), it follows that the above equation can be rewritten in terms of the basis functions as

$$\sum_K \sum_{j=1}^{n_{en}} c_j^K \{-(\nabla\psi_j, \nabla v_1)_K + k^2(\psi_j, v_1)_K + k^2(\varphi_j, v_1)_K = (f, v_1) - (h, v_1)_{\Gamma_2}\,. \tag{19}$$

Finally, setting $v_1 = \psi_i$ gives

$$\sum_K \sum_{j=1}^{n_{en}} c_j^K \{-(\nabla\psi_j, \nabla\psi_i)_K + k^2(\psi_j, \psi_i)_K + k^2(\varphi_j, \psi_i)_K = (f, \psi_i) - (h, \psi_i)_{\Gamma_2} \,. \tag{20}$$

To implement this formulation it is useful to consider the bubble shape functions rewritten as

$$\varphi_j = -\psi_j + \lambda_j \,, \tag{21}$$

where, from (6)-(7), λ_j solves

$$L\lambda_j = 0 \qquad \text{in}\, K \,, \tag{22}$$

$$\lambda_j = -\varphi_{j,K} \qquad \text{on}\, \partial K \,, \tag{23}$$

and from (20) the matrix formulation simplifies to solving

$$\sum_K \sum_{j=1}^{n_{en}} c_j^K \{-(\nabla\psi_j, \nabla\psi_i)_K + k^2(\lambda_j, \psi_i)_K = (f, \psi_i) - (h, \psi_i)_{\Gamma_2} \,. \tag{24}$$

For concreteness, we solve (22)-(23) on a square of side a, placed in the first quadrant of the Cartesian coordinates x-y. Thus, for the shape function ψ_j with value one at $x = y = a$ we solve

$$\Delta\lambda_j + k^2\lambda_j = 0 \qquad \text{in}\, K \,, \tag{25}$$

$$\lambda_j = 0 \qquad \text{on}\, x = 0\, \text{or}\, y = 0 \,, \tag{26}$$

$$\lambda_j = y/a \qquad \text{on}\, x = a \,, \tag{27}$$

$$\lambda_j = x/a \qquad \text{on}\, y = a \,. \tag{28}$$

By separation-of-variables we obtain the following exact solution

$$\lambda_j = \sum_{m=1}^{\infty} (-1)^{m+1} \frac{2}{m\pi \sinh(\sqrt{\frac{m^2\pi^2}{a^2} - k^2}\, a)} \left\{ \sin(\frac{m\pi x}{a}) \sinh(\sqrt{\frac{m^2\pi^2}{a^2} - k^2}\, y) + \sin(\frac{m\pi y}{a}) \sinh(\sqrt{\frac{m^2\pi^2}{a^2} - k^2}\, x) \right\} . \tag{29}$$

The formulas for the shape function ψ_j with value one at the other nodes are similar. Therefore, we are now able to substitute back into (24) and solve the system of equations using this residual-free-bubble approach.

Remark:

Clearly the derivation of the residual-free-bubbles here can be extended to, and is limited to, rectangular elements. For arbitrarily shaped elements, suitable approximations of the residual-free bubbles are in the works.

3. NUMERICAL EXPERIMENTS

In this section we evaluate the performance of the Residual Free Bubble Method, that we refer to as RF-bubbles. The performance of this method is compared with the GLS method as well as with the Galerkin method using piecewise bilinear functions. The GLS method with the definitions of the stabilization parameters presented in [8] is used in our examples.

3.1 2D Green's function problem

This problem is one of the test problems presented in [12]. As this case considers a singular load inside an element, it will be useful to assess the improved performance of our method when information inside the elements is relevant.

This test case consists of an unit square domain $\Omega = (0,1)\times(0,1)$, with homogeneous Dirichlet boundary conditions. The forcing function $f = \delta(x_0, y_0)$ is a Dirac delta function located at $(x_0, y_0) = (0.1875, 0.1875)$, which coincides with an element centroid. The non-dimensional wave number is $kL = 8$, and the domain is partitioned into a regular mesh of 8×8 square elements.

After the calculation of the global problem, the bubble is computed, and the solution is the sum of the bilinear part and the bubble term. In particular, for this singular load case, the bubble is able to capture accurately the spike resulting from this load.

First we compare the solution at $y_p = 0.190625$, which corresponds to a "cut" just a little above the point where the singular load is applied. Then we examine the behavior of the solution inside the elements. In Figure 1 we compare the RF-bubbles method with GLS and Galerkin solutions with bilinears for the same mesh. Note how the addition of the bubble inside the element in the RF-bubbles method improves the solution by capturing the spike caused by the singular load. We use 10 points in each element interior for this display of the bubble solution. 200 terms are used in the series expansion of the residual-free bubbles (Fewer terms could be used, but we are trying to assess accuracy

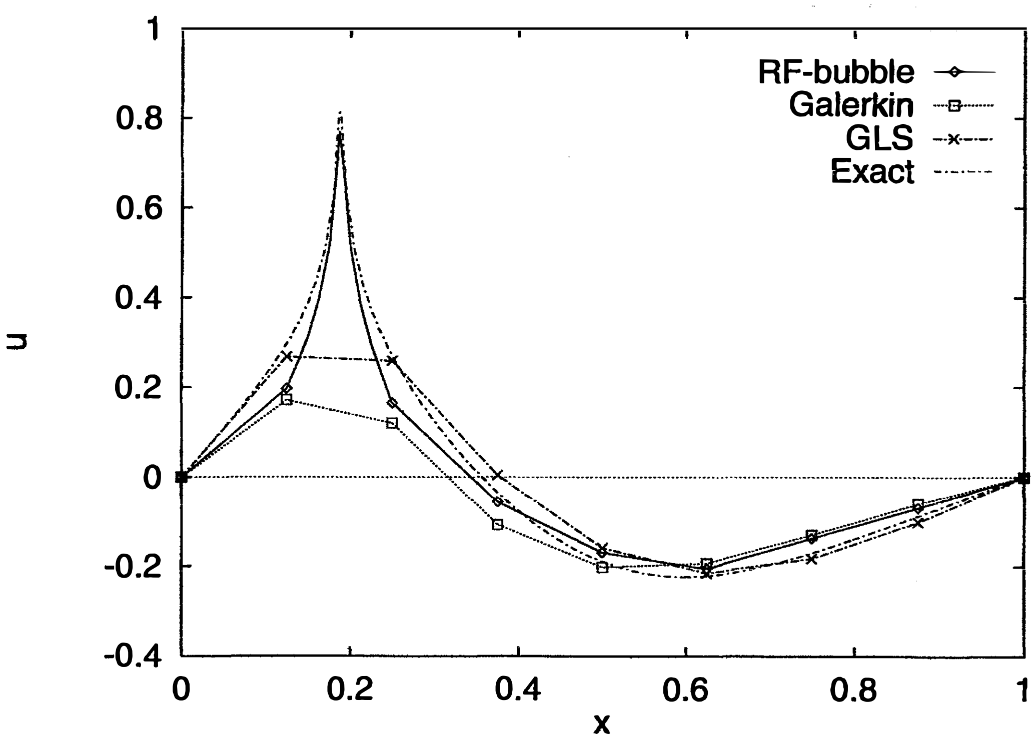

Figure 1: Singular load problem. Comparison at $y = y_p$

here). For this problem we also need to solve for an additional bubble due to the load (see equations (8)-(9)). The exact solution for this problem can be found in [12].

The bubble is able to capture the singularity well, and the improvement of the solution is apparent as displayed in Figure 2. The GLS solution with bilinears is unable to approximate well the singular response. Away from this region of the singularity all methods seem to perform well, but close to the spike the GLS method with bilin-

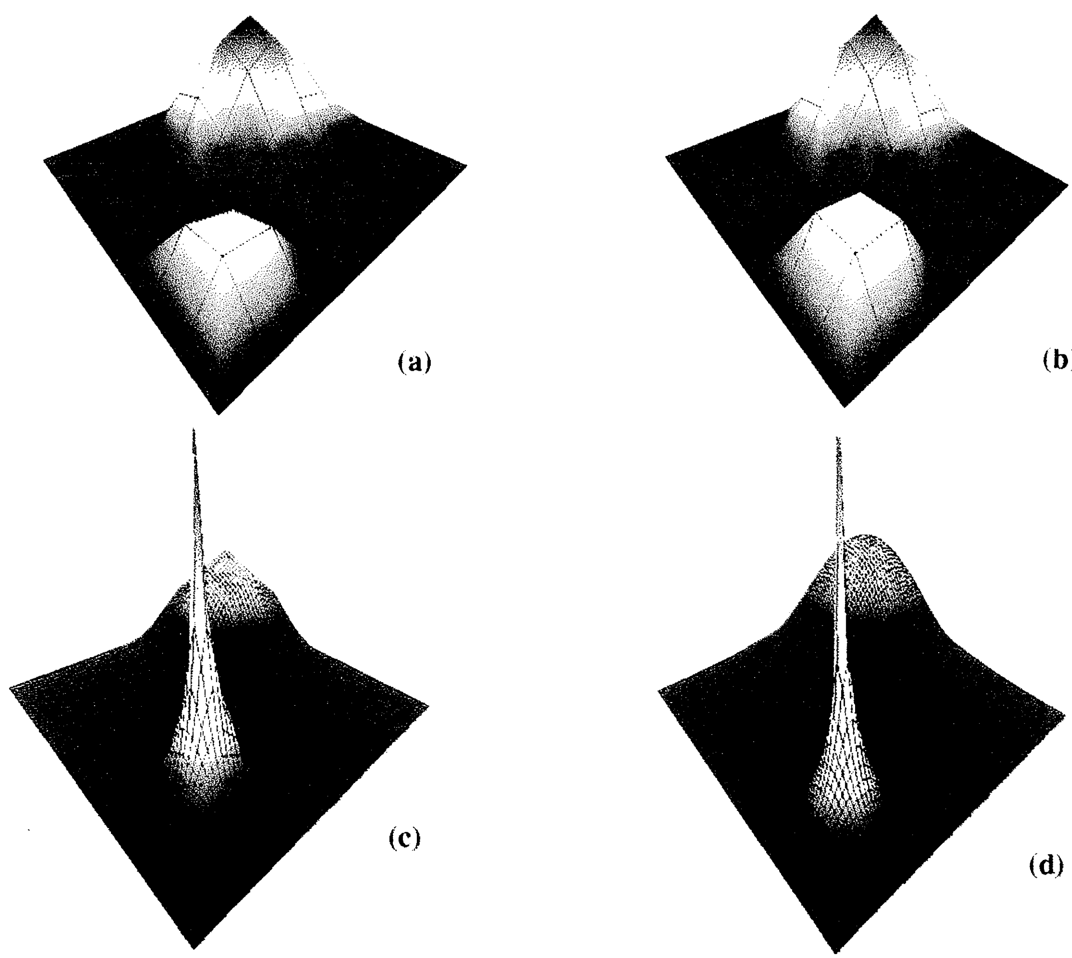

Figure 2: Singular load problem. Elevation plots for: a) RF-bubble solution without the bubbles; b) GLS; c) RF-bubble solution with the bubbles; d) The exact solution.

ears needs significant mesh refinement to capture the behavior of the exact solution.

3.2 Scattering in an L-shaped domain

We consider an L-shaped domain with homogeneous Dirichlet boundary conditions, except for a load on half of one of the faces of the L as shown in Figure 3.

For this problem, we perform a convergence study by comparing the performance of the Galerkin, GLS and RF-bubbles methods. The non-dimensional wave number is $kL = 8$, where L is the width of our L-shaped domain. All the meshes presented are

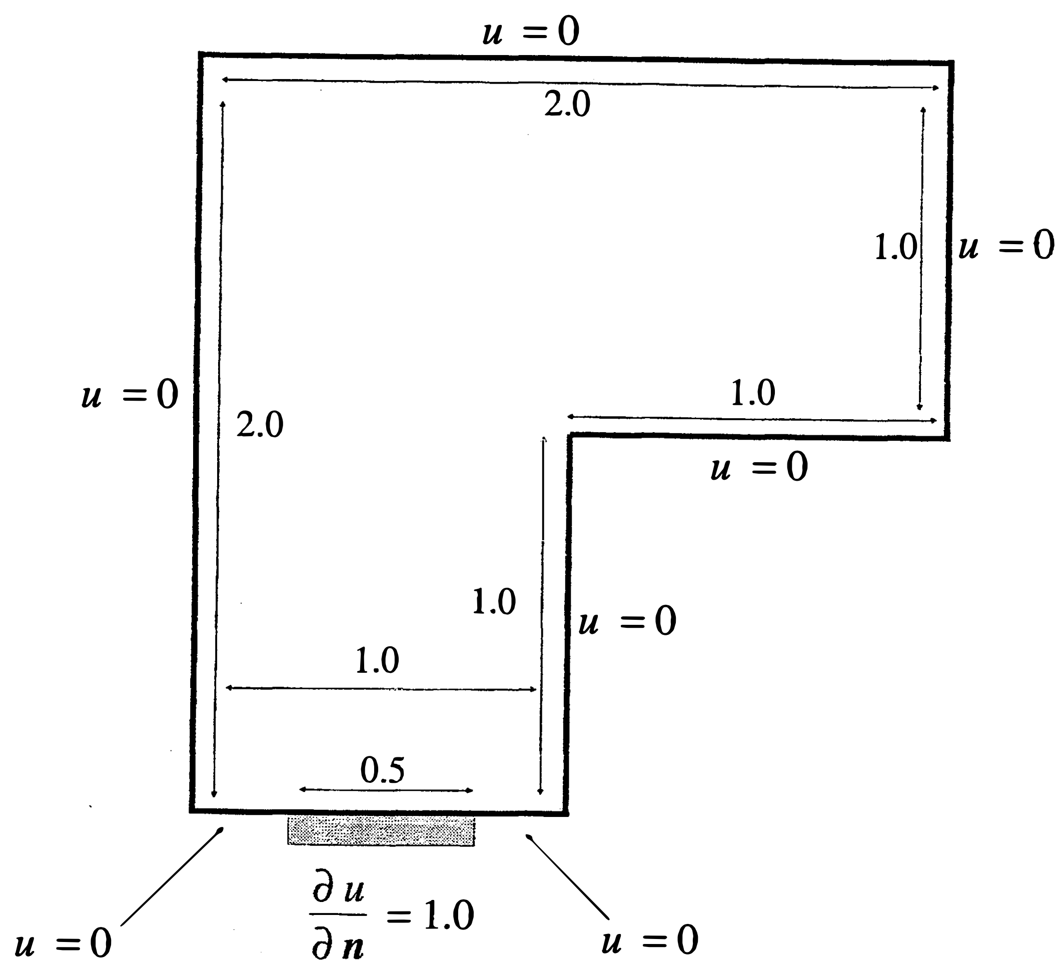

Figure 3: Scattering test case: problem statement

uniform and the number of elements displayed in the figure captions correspond to the number of elements in each of the three squares that make up the L-shaped domain.

In Figures 4 to 7 we plot the convergence study for this problem. The meshes in these figures are 4×4, 8×8, 16×16 and 32×32, respectively.

The results for the 4×4 mesh are poor for all methods, as shown in Figure 4, but the RF-bubbles method, with the addition of the bubble, presents a better performance, as it is able to represent well the phase characteristics of the converged solution (shown in Figure 7). The results of the 8×8 mesh are shown in Figure 5. We observe a poor performance of the Galerkin method, and the GLS method still presents a high phase error. The RF-bubbles starts to converge and represents phase quite well. For the next mesh, 16×16, in Figure 6 we can still see the bad performance of the Galerkin method, and we note that this solution looks like the RF-bubbles solution of the 4×4 mesh, as the Galerkin method only now starts to represent well the phase characteristics of the converged solution. For this mesh both the GLS and RF-bubbles perform well. For the 32×32 mesh (Figure 7), all methods converge and we have a good reference to evaluate the performance of the methods for intermediate meshes.

ACKNOWLEDGMENT

During the course of this work Charbel Farhat and Michel Lesoinne were partially supported by the Office of Naval Research under Grant N-00014-95-1-0663 and Antonini P. Macedo was partially supported by Brazilian Government fellowship CAPES Proc. 1233/95-2.

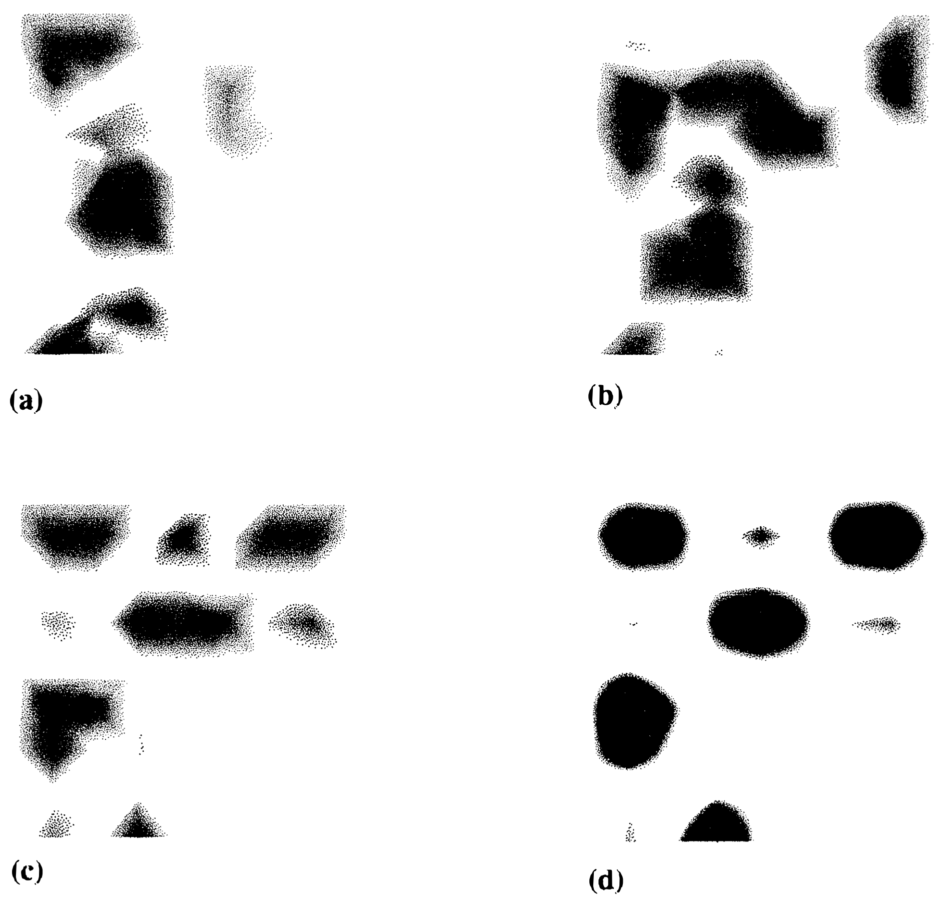

Figure 4. Scattering in an L-shaped domain with $3 \times (4 \times 4)$ squares: a) The Galerkin method with piecewise bilinears; b) The GLS method with piecewise bilinears; c) RF-Bubbles method without adding the bubbles; d) RF-Bubbles method adding the bubbles.

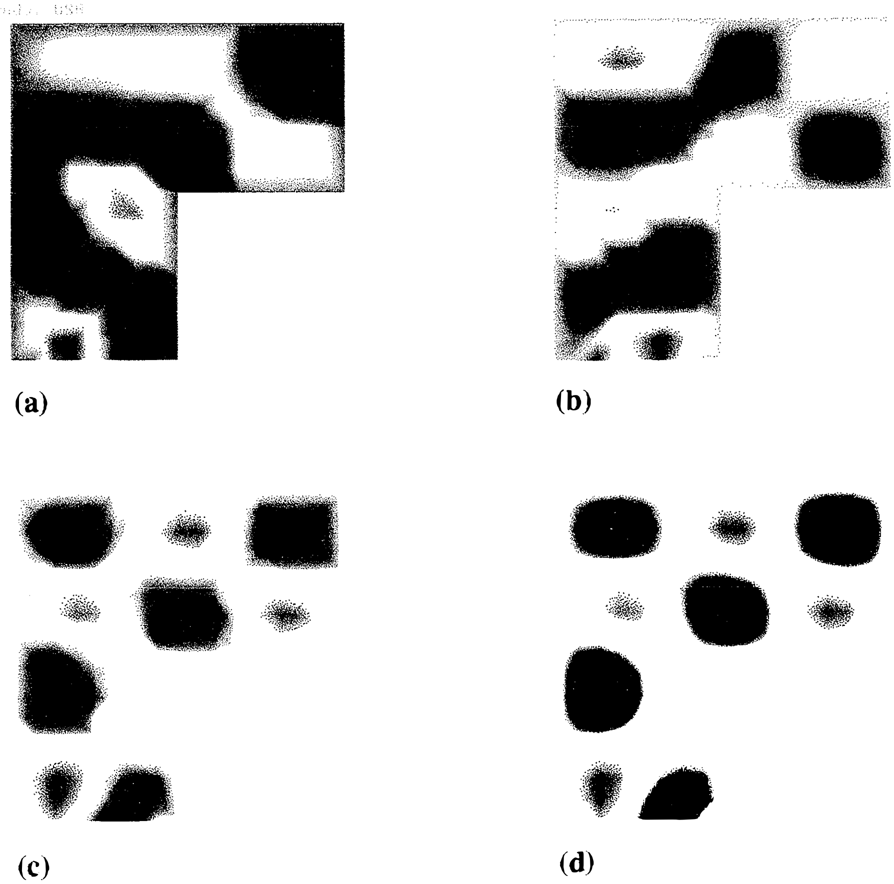

Figure 5. Scattering in an L-shaped domain with $3 \times (8 \times 8)$ squares: a) The Galerkin method with piecewise bilinears; b) The GLS method with piecewise bilinears; c) RF-Bubbles method without adding the bubbles; d) RF-Bubbles method adding the bubbles.

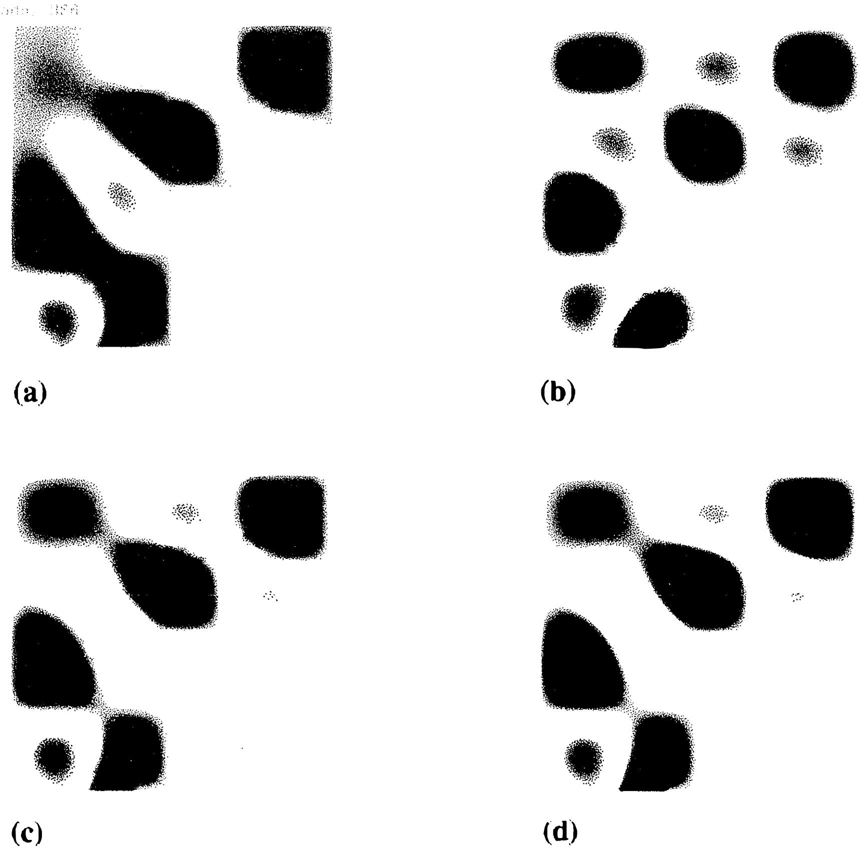

Figure 6. Scattering in an L-shaped domain with $3 \times (16 \times 16)$ squares: a) The Galerkin method with piecewise bilinears; b) The GLS method with piecewise bilinears; c) RF-Bubbles method without adding the bubbles; d) RF-Bubbles method adding the bubbles.

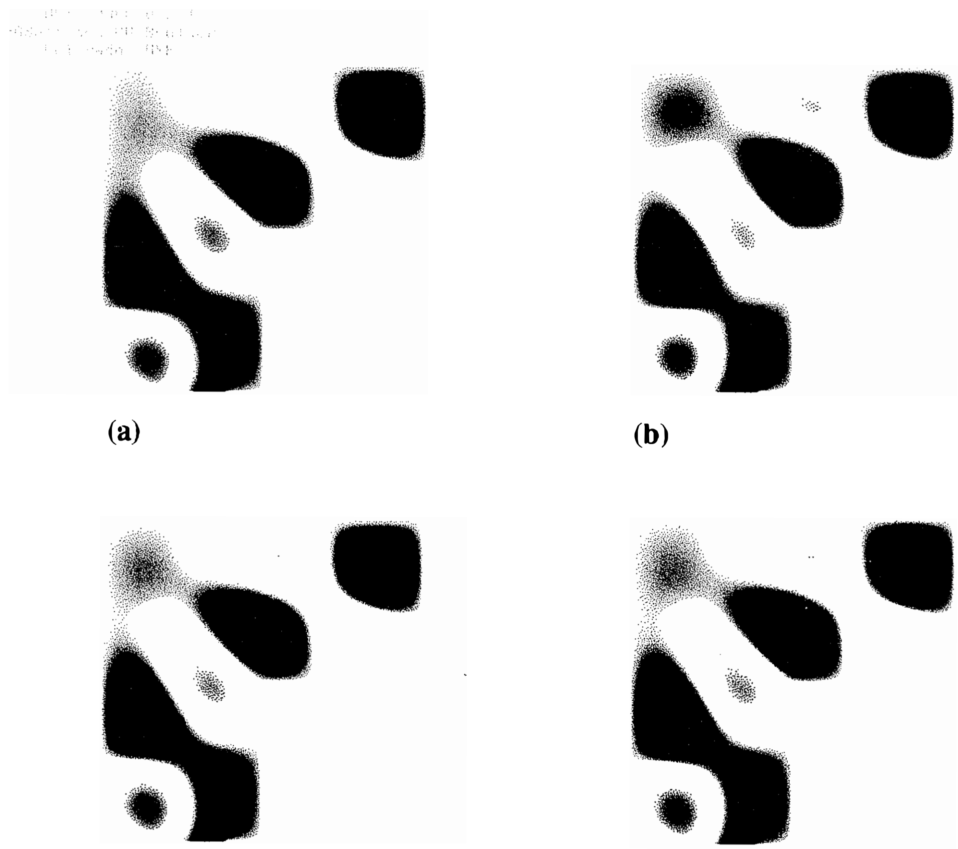

(a) (b) (c) (d)

Figure 7. Scattering in an L-shaped domain with $3 \times (32 \times 32)$ squares: a) The Galerkin method with piecewise bilinears; b) The GLS method with piecewise bilinears; c) RF-Bubbles method without adding the bubbles; d) RF-Bubbles method adding the bubbles.

REFERENCES

[1] I. Babuška, F. Ihlenburg, E.T. Paik and S.A. Sauter, "A generalized finite element method for solving the Helmholtz equation in two dimensions with minimal pollution," *Computer Methods in Applied Mechanics and Engineering*, Vol.**128** (1995) 325-359.

[2] F. Brezzi, L.P. Franca, T.J.R. Hughes and A. Russo, "$b = \int g$," *Computer Methods in Applied Mechanics and Engineering*, to appear.

[3] F. Brezzi and A. Russo, "Choosing bubbles for advection-diffusion problems," *Math. Models Meths. Appl. Sci.* Vol.**4** (1994) 571-587.

[4] L.P. Franca and T.J.R. Hughes, "Two classes of mixed finite element methods", *Comput. Methods Appl. Mech. Engrg.* Vol.**69** (1988) 89-129.

[5] L.P. Franca and A. Russo, "Deriving upwinding, mass lumping and selective reduced integration by residual-free bubbles," *Applied Mathematics Letters*, in press.

[6] L.P. Franca and A. Russo, "Mass lumping emanating from residual-free bubbles," *Computer Methods in Applied Mechanics and Engineering*, to appear.

[7] L.P. Franca and A. Russo, "Unlocking with residual-free bubbles," *Computer Methods in Applied Mechanics and Engineering*, to appear.

[8] I. Harari and T.J.R. Hughes, "Finite element methods for the Helmholtz equation in an exterior domain: model problems," *Computer Methods in Applied Mechanics and Engineering*, Vol.**87** (1991) 59-96.

[9] T.J.R. Hughes, "Multiscale phenomena: Green's functions, the Dirichlet-to-Neumann formulation, subgrid scale models, bubbles and the origin of stabilized

methods," *Computer Methods in Applied Mechanics and Engineering*, Vol.**127** (1995) 387-401.

[10] T.J.R. Hughes and L.P. Franca, "A new finite element formulation for computational fluid dynamics: VII. The Stokes problem with various well-posed boundary conditions: symmetric formulations that converge for all velocity/pressure spaces", *Comput. Methods Appl. Mech. Engrg.* Vol.**65** (1987) 85-96.

[11] T.J.R. Hughes, L.P. Franca and G.M. Hulbert, "A new finite element formulation for computational fluid dynamics: VIII. The Galerkin-least-squares method for advective-diffusive equations", *Comput. Methods Appl. Mech. Engrg.* Vol.**73** (1989) 173-189.

[12] A.A. Oberai and P.M. Pinsky, "A finite element method for the Helmholtz equation based on a subgrid scale model," in pp 79-85 of the Numerical Methods in Enginneering '96 - Proceedings of the Second ECCOMAS Conference on Numerical Methods in Engineering, 9-13 September 96, Paris, France, John Wiley & Sons, Chichester, 1996.

CENTER FOR COMPUTATIONAL MATHEMATICS REPORTS

University of Colorado at Denver
P.O. Box 173364, Campus Box 170
Denver, CO 80217-3364

Fax: (303) 556-8550
Phone: (303) 556-8442
http://www-math.cudenver.edu/

72. C. Liu, Z. Liu and G. Xiong, "Direct Numerical Simulation for the Receptivity and the Whole Process of Transition Around 2-D Airfoils."
73. R. Tezaur, P. Vaněk and M. Brezina, "Two-Level Method for Solids on Unstructured Meshes."
74. T.F. Russell, D.W. Dean, T.H. Illangasekare, R. Mapa and J. Garcia, "Upscaling of Dispersivity in Modeling of Solute Transport: Mathematical Theory and Laboratory Experiments."
75. T.F. Russell, R.W. Healy, R.G. Striegl, G.L. Hutchinson and G.P. Livingston, "Analytical Solution for the Problem of 1-Dimensional Diffusion into a Static Chamber."
76. T.F. Russell and R.V. Trujillo, "The Finite Volume Element Method For Elliptic and Parabolic Equations."
77. R.W. Healy and T.F. Russell, "Solution of the Advection-Dispersion Equation in Two Dimensions by a Finite-Volume Eulerian-Lagrangian Localized Adjoint Method."
78. Z. Cai, R.R. Parashkevov, T.F. Russell and X. Ye, "Domain Decomposition for a Mixed Finite Element Method in Three Dimensions."
79. S.E. Payne, T. Pentilla and G.F. Royle, "Building a Cyclic q-Clan."
80. K.D. Jamison and W.A. Lodwick, "Minimizing Unconstrained Fuzzy Functions."
81. F. Brezzi, L.P. Franca, T.J.R. Hughes and A. Russo, "$b = \int g$."
82. L.P. Franca, C. Farhat, M. Lesoinne and A. Russo, "Unusual Stabilized Finite Element Methods and Residual-Free-Bubbles."
83. F. Brezzi, L.P. Franca, T.J.R. Hughes and A. Russo, "Stabilization Techniques and Subgrid Scales Capturing."
84. J. Mandel, R. Tezaur and C. Farhat, "A Scalable Substructuring Method by Lagrange Multipliers for Plate Bending Problems."
85. K. Kafadar, P.C. Prorok and P.J. Smith, "An Estimate of the Variance of Estimators for Lead Time and Screening Benefit in Randomized Cancer Screening Trials."
86. H.J. Greenberg, "Rim Sensitivity Analysis from an Interior Solution."
87. K. Kafadar, "Two-Dimensional Smoothing: Procedures and Applications to Engineering Data."